Diet-induced obesity causes peripheral and central ghrelin resistance by promoting inflammation

Farhana Naznin[1], Koji Toshinai[1], T M Zaved Waise[1], Cherl NamKoong[1], Abu Saleh Md Moin[1], Hideyuki Sakoda[1], Masamitsu Nakazato[1, 2]

[1]Division of Neurology, Respirology, Endocrinology and Metabolism,
Department of Internal Medicine, Faculty of Medicine, University of Miyazaki,
5200 Kihara, Kiyotake, Miyazaki 889-1692, Japan

[2]CREST (Japan) Agency for Medical Research and Development (A-MED)
1-2-2 Kasumigaseki, Chiyoda-ku, Tokyo 100-8916, Japan

Correspondence should be addressed to Masamitsu Nakazato, M.D., Ph.D.
E-mail: nakazato@med.miyazaki-u.ac.jp

Keywords: ghrelin, diet-induced obesity, nodose ganglion, vagus nerve, inflammation
Word count:4,205

Abstract

Ghrelin, a stomach-derived orexigenic peptide, transmits starvation signals to the hypothalamus via the vagus afferent nerve. Peripheral administration of ghrelin does not induce food intake in high fat diet (HFD)-induced obese mice. We investigated whether this ghrelin resistance was caused by dysfunction of the vagus afferent pathway. Subcutaneous ghrelin administration did not induce food intake, suppression of oxygen consumption, electrical activity of the vagal afferent nerve, phosphorylation of extracellular-signal-regulated kinases 2 (ERK2) and AMP-activated protein kinase α (AMPKα) in the nodose ganglion, or Fos expression in hypothalamic arcuate nucleus of mice fed a HFD for 12 weeks. Administration of anti-ghrelin IgG did not induce suppression of food intake in HFD-fed mice. Expression levels of ghrelin receptor mRNA in the nodose ganglion and hypothalamus of HFD-fed mice were reduced. Inflammatory responses, including upregulation of macrophage/microglia markers and inflammatory cytokines, occurred in the nodose ganglion and hypothalamus of HFD-fed mice. A high-fat diet blunted ghrelin signaling in the nodose ganglion via a mechanism involving *in situ* activation of inflammation. These results show that ghrelin resistance in the obese state may be caused by dysregulation of ghrelin signaling via the vagal afferent.

1. Introduction

Control of food intake in the brain is regulated by the integration of both the neuronal and humoral signals from the periphery. A variety of sensory information derived from the gastrointestinal tract is transmitted to the nucleus of the tractus solitaries (NTS) in the medulla oblongata via the vagal afferent nerve, terminating in hypothalamic nuclei implicated in the control of feeding (Rinaman 2010). The nodose ganglion, located outside the jugular foramen, is a constellation of vagal afferent neurons that synthesize receptors for gut peptides that regulate feeding and energy homeostasis (Konturek *et al*. 2004, Zhuo *et al.* 1997). These receptors are transported to afferent terminals in the gastrointestinal mucosa, which are more optimally positioned to monitor bioactive substances released from gastrointestinal enteroendocrine cells. Nodose ganglion neurons are pseudounipolar neurons with two axons running towards the visceral organs and the NTS.

Ghrelin, a peptide primarily produced in the stomach, stimulates feeding (Kojima *et al.* 1999, Nakazato *et al.* 2001). Ghrelin exists in two major forms, n-octanoyl-modified ghrelin and desacyl-ghrelin (a non-acylated form of ghrelin). Biosynthesis of ghrelin is downregulated in obesity, and fasting plasma ghrelin concentrations in humans are negatively correlated with body weight, percentage body fat, and fat mass (Shiiya *et al*. 2002, Tschöp *et al*. 2001). The growth-hormone secretagogue receptor (GHSR), also known as the ghrelin receptor, is synthesized in vagal afferent neurons and transported to the stomach by axonal transport (Date *et al*. 2002). Ghrelin binds to this receptor and suppresses the electrical activity of the gastric vagal afferent. This information is transmitted to the NTS and relayed via the noradrenergic pathway to the hypothalamic neurons expressing orexigenic neuropeptides, neuropeptide Y (NPY) and agouti-related peptide (AgRP) (Date *et al.* 2006). Diet-induced obesity (DIO) causes resistance to central administration of ghrelin by suppressing expression of the ghrelin receptor in NPY/AgRP neurons (Briggs *et al.* 2010).

Peripheral administration of ghrelin also failed to induce feeding in DIO mice (Briggs *et al.* 2010); however, the mechanism underlying this unresponsiveness remains to be demonstrated.

Immune cell–mediated tissue inflammation in the adipose tissue, liver, and skeletal muscle plays a critical role in the development of obesity and insulin resistance (Hotamisligil *et al.* 1993, Schenk *et al*. 2008). Obesity-associated inflammation, including enhanced expression of interleukin (IL)-1β, tumor necrosis factor (TNF)-α, and IL-6 in the hypothalamus, was first reported in 2005 (De Souza *et al.* 2005), and many investigators have since replicated this finding (Cai and Liu 2011, Thaler *et al.* 2013). Diet-induced obesity attenuated both sensitivities of vagal afferents to the satiety mediators and membrane excitability of vagal afferents (Daly *et al*. 2011), suggesting that the development of obesity may be related to impairments in the vagal afferent system.

We studied ghrelin's effects on feeding, energy consumption, electrical activation of the vagus afferent, and neuronal activation in the hypothalamus of DIO mice fed a high fat diet (HFD) for 12 weeks. Expression of the ghrelin receptor in both the nodose ganglion and hypothalamus were downregulated in HFD-fed mice. Ghrelin stimulated phosphorylation of extracellular-signal-regulated kinases 2 (ERK2) and AMP-activated protein kinase α (AMPKα) in the nodose ganglion in chow diet (CD)-fed mice, but not HFD-fed mice. Microglia/macrophages represent the first line of immune defense in both the central and peripheral nervous systems. Therefore, we also investigated inflammation in the nodose ganglion and hypothalamus by performing immunohistochemistry of macrophages/microglia and mRNA expression profiling of inflammatory cytokines. We conclude that DIO causes inflammatory responses in the nodose ganglion and ghrelin resistance in the vagal afferent system.

2. Materials and methods

Animals

Male C57BL/6J mice (6-week-old male, 20–21 g, Charles River Laboratories, Yokohama, Japan) were maintained in individual cages under controlled temperature (21–23°C) and light (light on: 08:00–20:00) conditions. They were maintained on either CD (12.3% fat, 59.2% carbohydrate, 28.5% protein, 14.2 kJ/g; CLEA Rodent Diet CE-2, CLEA Japan, Tokyo, Japan) or HFD (60% fat, 20% carbohydrate, 20% protein, 21.9 kJ/g; no.D12492; Research Diets, New Brunswick, NJ, USA) with free access to food for 12 weeks. All animal experiments were performed in accordance with the Japanese Physiological Society's guidelines for animal care. Intracerebroventricular (i.c.v.) cannulae were implanted into the lateral cerebral ventricle under anesthesia by intraperitoneal (i.p.) injection of sodium pentobarbital (Abbot Laboratories, Chicago, IL, USA). Only animals demonstrating progressive weight gain after the surgery were used in subsequent experiments.

Characteristics of HFD-fed mice

Mice fed CD or HFD for 12 weeks (n = 8 per group) were fasted from 09:00 to 14:00, and then blood was collected by tail-prick. Blood glucose was measured with a glucometer (Terumo, Tokyo, Japan), and plasma insulin was measured using a mouse insulin EIA kit (Morinaga Institute of Biological Science, Yokohama, Japan). For plasma ghrelin and leptin measurements, CD- or HFD-fed mice were deeply anesthetized with sodium pentobarbital, and blood samples were collected by cardiac puncture. Plasma ghrelin was measured using an active ghrelin ELISA Kit (Mitsubishi Chemical Medience, Tokyo, Japan) and des-acyl ghrelin with a des-acyl ghrelin ELISA Kit (Mitsubishi Chemical Medience). Plasma leptin was measured using a mouse/rat leptin ELISA kit (Morinaga Institute of Biological Science). Amount of daily food intake was measured for 4 days before the administration experiments. Epididymal fat weight was measured at sacrifice.

Food intake experiments

Mice fed CD or HFD (n = 6 per group) for 11 weeks were transferred to single cages and maintained for 1 week, during which they were acclimatized by subcutaneous (s.c.) injections of saline once daily for 3 days. First, mice were subcutaneously administered ghrelin (60 nmol/kg BW; Peptide Institute, Osaka, Japan) or saline. Second, mice (n = 6 per group) received an i.c.v. injection of artificial cerebrospinal fluid (aCSF) or ghrelin (500 pmol). Administration was performed at 10:00 in both experiments, and 2-h food intake was measured. Third, mice (n = 6 per group) received an i.c.v. injection of anti-ghrelin IgG (0.5 µg/2 µl aCSF) prepared elsewhere (Nakazato *et al*. 2001) or normal rabbit serum IgG (0.5 µg/2 µl aCSF) at 18:00. Fourth, mice (n = 6 per group) received an i.p. injection of leptin (2 µg/g BW; Sigma-Aldrich, St Louis, MO, USA) or saline at 20:00. Dark-phase food intake was measured in the third and fourth experiments. Ghrelin was dissolved in 50 µl saline for s.c. administration, and in 2 µl aCSF for i.c.v. administration.

Oxygen consumption

Mice fed CD or HFD (n = 4 per group) for 11 weeks were housed in a metabolic chamber (Shinfactory, Fukuoka, Japan) for 1 week. They were given s.c. injection of ghrelin (60 nmol/kg BW) or saline at 10:00, and then returned to the chambers. Oxygen consumption was measured in an Oxymax (Columbus Instruments, Columbus, OH, USA) for 120 min. Mice were deprived of food during the measurement.

Pharmacokinetics of s.c. administration of ghrelin

Mice fed CD or HFD (n = 3 per group) were subcutaneously administered ghrelin (60 nmol/kg BW). Blood was taken from the tail vein 0, 15, 30, 60, and 120 min after administration and immediately collected into tubes containing disodium EDTA (1 g/l) with aprotinin (500 kIU/l) (Wako Pure Chemicals, Osaka, Japan). Plasma was mixed with 1 M HCl (10% of plasma volume). Ghrelin was measured using an active ghrelin ELISA kit.

Electrophysiology study

Multiunit neural discharge in gastric vagal afferent fibers was recorded extracellularly. CD- or HFD-fed mice were anesthetized by an i.p. injection of urethan (1 g/kg) (Sigma-Aldrich). For electrophysiological studies, animals were anesthetized throughout the procedure. Standard methods of extracellular recording from vagal nerve filaments were used, as described in detail elsewhere (Date *et al*. 2005). We placed filaments isolated from the gastric branch of the vagal trunk peripheral, cut under the diaphragm for recording of afferent nerve activity, on a pair of silver wire electrodes. Silver wire electrodes, connected through a Differential Extracellular Amplifier (ER-1; Cygnus Technology, Delaware Water Gap, PA, USA) to a PowerLab/8SP (ADInstruments, Melbourne, Australia), were used to record neural activity. The number of spikes was calculated using the Labchart 7 software (ADInstruments) with a rate meter. After 10 min recording of basal nerve discharges from the multiunit afferents, these nerve discharges were continually recorded for 15 min after s.c. administration of saline or ghrelin (60 nmol/kg BW) (n = 4 per group) in CD- or HFD-fed mice. The total number of spikes for 15 min after administration was calculated.

Fos expression

Mice (n = 3 per group) received an i.c.v. administration of ghrelin (500 pmol/2 µl aCSF), a s.c. administration of ghrelin (60 nmol/kg BW), or saline 90 min before transcardial perfusion with 4% paraformaldehyde. They were anesthetized with sodium pentobarbital and transcardially perfused with ice-cold heparinized 0.1 M phosphate buffer (PB, pH 7.4) for 20 min, and then with ice-cold 4% paraformaldehyde in PB for 20 min. The brain was removed and post-fixed overnight in the fixative solution containing 4% paraformaldehyde, and then cryoprotected in 0.1 M PB containing 20% sucrose. We cut 40-µm sections of the hypothalamus. Fos immunohistochemistry the method was performed as described elsewhere (Toshinai *et al.* 2003). Briefly, free-floating sections were incubated in 0.3% hydrogen

peroxide for 10 min, blocked with 1% normal goat antiserum (Santa Cruz Biotechnology, Dallas, TX, USA), and incubated in rabbit Fos antiserum (1:500 dilution, Santa Cruz Biotechnology) in 0.01 M phosphate buffer saline (PBS, pH 7.4) overnight at 4°C with gentle agitation. Sections were then incubated in biotinylated goat anti-rabbit IgG (1:500 dilution, Vector Laboratories, Burlingame, CA, USA), and immunoreactivity was visualized using the avidin–biotin–peroxidase complex reaction method with diaminobenzimide (VECTASTAIN Elite kit, Vector Laboratories). Fos-positive cells were automatically counted in the sections using a cell-counting program (Bio-Imaging Analysis System Lumina Vision, Tokyo, Japan).

Real-time polymerase chain reaction (RT-PCR)

The nodose ganglion and hypothalamus were removed from anesthetized CD- or HFD-fed mice. Total RNA was extracted with a RiboPure™ kit (Ambion, Austin, TX, USA). RT-PCR was conducted on a LightCycler system (Roche Diagnostics, Mannheim, Germany) using SYBR Premix Ex Taq (2×) (Takara Bio, Shiga, Japan) and the following primer sets: mouse *Ghsr*, ATCACCTCTGGGTCTTGTTGCTG and GCTGAATGGCTCATTGTAGTCCTG; ionized calcium binding adapter molecule (*Iba1*), AGCTGCCTGTCTTAACCTGCATC and TTCTGGGACCGTTCTCACACTTC; Egf-like module-containing, mucin-like, hormone receptor-like 1 (*Emr1)*, GAGATTGTGGAAGCATCCGAGAC and GACTGTACCCACATGGCTGATGA; *Il6*, CCACTTCACAAGTCGGAGGCTTA and CCAGTTTGGTAGCATCCATCATTTC; *Il1b*, TCCAGGATGAGGACATGAGCAC and GAACGTCACACACCAGCAGGTTA; *Tnfα*, TATGGCCCAGACCCTCACA and GGAGTAGACAAGGTACAACCCATC; Toll-like receptor 4 (*Tlr4)*, GGAAGTTCACATAGCTGAATGAC and CAAGGCATGTCCAGAAATGAGA; toll-like receptor 2 (*Tlr2)*, TGTCTCCACAAGCGGGACTTC and TTGCACCACTCGCTCCGTA; *Tbp*, CATTCTCAAACTCTGACCACTGCAC and CAGCCAAGATTCACGGTAGATACAA; and

188 *Gapdh*, TCAAGAAGGTGGTGAAGCAG and TGGGAGTTGCTGTTGAAGTC. The
189 obtained values were normalized against that of *Gapdh* or *Tbp*, used as an internal control.

190 ***Immunohistochemistry***

191 Nodose ganglia and whole brains (n = 4 per group) were immersed in 4%
192 paraformaldehyde/PB for 24 h at 4°C, incubated for 24 h in PB containing 20% sucrose,
193 quickly frozen on dry ice, and cut into 8-μm slices with a cryostat at −20°C. Sections blocked
194 for 5 min in protein-block serum-free solution (Dako, Carpinteria, CA, USA) were incubated
195 overnight at 4°C with rabbit anti-Iba1 (1:10,000; Wako Pure Chemicals), rat anti-CD11b
196 (1:50; AbD Serotec, Oxford, UK), and rat anti-CD86 (1:100; Abcam, Cambridge, UK).
197 Immunofluorescence was performed with a combination of Alexa Fluor 488–labeled anti-
198 rabbit secondary antibody or Alexa Fluor 594–labeled anti-rat secondary antibody (both
199 1:400; Invitrogen, Carlsbad, CA, USA). Images were captured on an OLYMPUS AX-7
200 fluorescence microscope (Olympus, Tokyo, Japan). Cells immunostained with Iba1, CD11b,
201 or CD86 antibody were counted manually with Olympus cellSens imaging software
202 (Olympus). Quantitation was performed in a blinded fashion.

203 ***Western blotting***

204 Mice (n = 6 per group) fed a CD or HFD for 12 weeks were anesthetized and injected
205 subcutaneously with ghrelin (60 nmol/kg BW) or saline. They were perfused with PB 60 min
206 later for AMPKα measurement, or 120 min later for ERK1/2 measurement, then the nodose
207 ganglion was isolated. Protein (10 to 20 μg) extracted from the nodose ganglion was
208 separated on SDS-PAGE Tris-glycine gels (Mini-PROTEAN®TGX™ Precast Gels, Bio-
209 RAD, Hercules, CA, USA) for 100 min at 75 V and transferred to nitrocellulose membrane.
210 Membranes were blocked with 5% (w/v) non-fat dry milk and incubated with antibodies for
211 phosphorylated Erk1/2 (Thr^{202}/Thr^{204}) (1:4000), Erk1/2 (1:4000), pAMPKα (1:2000),
212 AMPKα (1:2000), or Gapdh (1:5000) (all five from Cell Signaling Technology Japan, Tokyo,

Japan) in blocking buffer overnight at 4°C. Membranes were then incubated with the corresponding secondary antibodies. For sequential analysis of membranes, bound antibodies were removed with stripping buffer (10% SDS, 1 M Tris-HCl, pH6.8) for 30 min at 55°C. After washes, membranes were developed in enhanced chemiluminescence buffer (ImmunoStar® LD, Wako Chemicals USA, Richmond, VA, USA) for 1 min. Densitometry was performed on the lanes using the GeneTools software (Syngene, Cambridge, UK) to quantitate protein expression. Band intensities were normalized by calculating the respective ratios of the intensities of the bands of pERK to ERK or pAMPKα to AMPKα.

Statistical analysis

Statistical analyses were performed by one- or two-way ANOVA followed by a Bonferroni's post-test for multiple comparisons, as appropriate. When two mean values were compared, analysis was performed by Mann–Whitney test or Wilcoxon or unpaired *t*-test. All data are expressed as means ± S.E.M. $P < 0.05$ was considered to be statistically significant.

3. Results

Characterization of HFD-fed mice

Table 1 shows characteristics and blood parameters in mice fed a HFD for 12 weeks. Food intake amount in HFD-fed mice was significantly lower than in CD-fed mice, whereas energy intake in the former was significantly higher. Body weights and epididymal fat weights in HFD-fed mice were higher than those in CD-fed mice. HFD caused significant increases in fasting blood glucose, plasma insulin and leptin, and decreases in plasma ghrelin and des-acyl ghrelin.

Ghrelin and leptin responses

Both s.c. and i.c.v. administrations of ghrelin enhanced food intake in CD-fed mice, but not HFD-fed mice (Fig. 1A and B). Inversely, i.c.v. administration of anti-ghrelin IgG

suppressed dark-phase food intake in CD-fed mice, but not HFD-fed mice (Fig. 1C). Subcutaneous administration of ghrelin reduced oxygen consumption in CD- but not HFD-fed mice (Fig. 1D, E, and F). Leptin administration did not reduce food intake in HFD-fed mice (Fig. 1G).

Pharmacokinetics of ghrelin

We compared time courses of plasma concentrations of ghrelin administered subcutaneously to CD- or HFD-fed mice (Fig. 2). The time courses of plasma ghrelin disappearance were similar between the two groups.

No effect of ghrelin on vagal afferent activity in HFD-fed mice

A representative record of the vagal afferent electrical activity in response to saline or ghrelin administration is shown in Figure 3. Ghrelin attenuated the vagal afferent nerve activity in CD- but not HFD-fed mice (Fig. 3A, B, C, and D). Ghrelin-induced suppression of the number of spikes was abrogated in HFD-fed mice (Fig. 3E).

Fos expression

Both s.c. and i.c.v. administrations of ghrelin caused a significant increase in the numbers of Fos-immunoreactive neurons in the hypothalamic arcuate nucleus of CD- but not HFD-fed mice (Fig. 4).

Ghsr mRNA expression

In HFD-fed mice, the *Ghsr* mRNA levels in the nodose ganglion and hypothalamus were significantly lower than those in CD-fed mice (Fig. 5).

Inflammatory mRNA and immunohistochemistry

TLR4 expression was significantly higher in HFD-fed mice than in CD-fed mice in the nodose ganglion, but not in the hypothalamus (Fig. 6A). In both groups, we observed no significant difference in the expression of TLR2 in the nodose ganglion or hypothalamus (Fig. 6B). The *Iba1*, *Il6*, and *Tnfα* mRNAs were significantly upregulated in the nodose ganglion

in HFD-fed mice relative to CD-fed mice (Fig. 6C). Hypothalamic expressions of mRNAs of *Iba1*, *Il6*, and *Tnfα* were also significantly upregulated in HFD-fed mice relative to CD-fed mice (Fig. 6D). The numbers of macrophages stained with anti-Iba1 (Fig. 6E and F) or anti-CD11b (Fig. 6G and H) antibodies in the nodose ganglion, as well as those stained with anti-Iba1 (Fig. 6I and J) or anti-CD11b (Fig. 6K and L) antibodies in the hypothalamus of HFD-fed mice, were significantly higher than those in CD-fed mice (Fig. 6M and N). Expression levels of the M1 macrophage markers Iba1 and CD86 in the nodose ganglion (Fig. 7A, B, D, and E) and hypothalamus (Fig. 7G, H, J, and K) of HFD-fed mice were significantly higher than those in CD-fed mice (Fig. 7M and N). Approximately 30% of Iba1-positive macrophages/microglia expressed CD86 immunoreactivity both in the nodose ganglion (Fig. 7C and F) and hypothalamus (Fig. 7I and L) of HFD-fed mice.

Effects of ghrelin on phosphorylations of ERK1/2 and AMPKα

ERK1/2 and pERK1/2 were detected in the nodose ganglion of both CD- and HFD-fed mice (Fig. 8A). HFD did not affect the phosphorylation of either ERK1 or ERK2, normalized against the corresponding total ERK level (Fig. 8B). Ghrelin administration significantly increased pERK2 in CD- but not HFD-fed mice (Fig. 8C).

The basal level of AMPKα in the nodose ganglion of HFD-fed mice was significantly higher than that in CD-fed mice (Fig. 9A and B). Ghrelin administration significantly increased pAMPKα in CD- but not HFD-fed mice (Fig. 9B).

4. Discussion

In this study, we showed that peripheral ghrelin resistance is associated with inflammation in the nodose ganglion, resulting in an impairment of the vagal afferent system. Previous studies showed that both peripheral and central administrations of ghrelin were unable to stimulate food intake in HFD-fed mice (Briggs *et al*. 2010, Gardiner *et al.* 2010,

Perreault *et al.* 2004). Here, we confirmed these findings in mice given 12-week HFD, in which 60% of the energy was provided as fat. Moreover, subcutaneous administration of ghrelin did not evoke suppression of vagal afferent activity, phosphorylation of ERK2 and AMPKα in the nodose ganglion, or Fos expression in the hypothalamic arcuate nucleus. We also showed that ghrelin neutralization by the i.c.v. administration of anti-ghrelin IgG failed to suppress natural feeding in DIO mice, suggesting that endogenous ghrelin did not act as an orexigenic peptide under HFD. A high-fat diet caused central ghrelin resistance by reducing both *Ghsr* expression in the hypothalamus and NPY/AgRP neuronal responsiveness to ghrelin (Briggs *et al*. 2010). Based on these findings, along with the upregulation of ghrelin secretion upon fast and downregulation of its secretion after meals, ghrelin is considered not to promote obesity, but rather to prevent starvation (Andrews *et al*. 2010, McFarlane *et al.* 2014). In this study, the disappearance of plasma ghrelin after its administration to HFD-fed mice was similar to that of CD-fed mice, indicating that the pharmacokinetics of ghrelin in DIO mice did not account for ghrelin resistance. The vagal afferent nerve is the major pathway conveying ghrelin's signals for starvation to the brain (Date *et al*. 2002). We postulated that downregulation of *Ghsr* expression in the nodose ganglion of DIO mice could blunt transmission of gastric-derived ghrelin's signals.

Several lines of evidence demonstrated that HFD activates an inflammatory response in the systemic organs and hypothalamus of rodents and humans (De Souza *et al.* 2005, Milanski *et al*. 2009, Posey *et al.* 2009). Hypothalamic inflammation induced by a HFD-manifested neuronal injury triggers a reactive gliosis by microglia and astrocytes (Thaler *et al*. 2012). These cellular responses occur selectively in the hypothalamic arcuate nucleus, a target region of gastric-derived ghrelin's signals. We postulated that HFD also caused inflammatory changes in the nodose ganglion. The calcium-binding protein Iba1 is a marker of microglia/macrophage activation in the nervous system (Ito *et al*. 1998). CD11b is another

marker of microglia/macrophage activation/recruitment (Perego *et al.* 2011). In this study, HFD induced macrophage activation and inflammatory responses in the nodose ganglion, as assessed by the increased numbers of Iba1- and CD11b-positive macrophages and production of inflammatory cytokines such as *Iba1*, *Il6*, and *Tnfα*. CD86, an activating and costimulatory protein, is expressed in activated microglia (Henkel *et al.* 2006). We also found that abundant $Iba1^{+}$ microglia expressed CD86, a marker of M1 macrophage/microglia. They were morphologically rounded and more ramified, suggesting that more activated subtypes of macrophages/microglia were present. HFD stimulated luminal lipopolysaccharide (LPS) production and TLR4 activation in colonic epithelial cells, thereby stimulating *in situ* inflammatory signaling (de La Serre *et al*. 2010). Vagal afferent nerve terminals innervating the gut are in close proximity to the LPS release site, and could therefore be involved in the mechanism underlying LPS signaling occurs. Lipopolysaccharide enhanced expression of SOCS3, a negative regulator of leptin-induced phosphorylation of STAT3 in nodose ganglion neurons, thereby causing leptin resistance in vagal afferent neurons (de Lartigue *et al*. 2011). Several lines of evidence suggest that the vagal afferent nerve transmits gut-derived inflammatory signals to the brain (Goehler *et al.* 1999, Hosoi *et al*. 2005). Further investigation is needed to determine whether HFD-induced TLR4 activation in the gut transmits inflammatory signals to the nodose ganglion via the vagal afferent.

The reported mechanisms by which ghrelin exerts its biological activities are complex. Ghrelin activates mitogen-activated protein kinases, including ERK1/2 (Mousseaux *et al.* 2006). ERK1/2 are protein-serine/threonine kinases involved in the activation of nuclear transcription factors controlling proliferation, differentiation, and cell death (Gutkind 2000). In our hands, ghrelin administration to CD-fed mice, but not HFD-fed mice, induced ERK2 phosphorylation in the nodose ganglion. The reduced expression of the GHSR in DIO mice could result in the downregulation of the GHSR-mediated ERK-signaling pathway in the

338 vagal afferent system.

339 AMPK is a key regulatory enzyme in cellular energy balance. Changes in
340 hypothalamic AMPK activity regulate food intake (Minokoshi *et al.* 2004), and ghrelin
341 activates hypothalamic AMPK (Kola *et al.* 2005). In this study, ghrelin administration to CD-
342 fed mice induced AMPK phosphorylation in both the nodose ganglion and hypothalamus, but
343 had no effect either tissues in DIO mice. We observed no difference between HFD and CD in
344 basal AMPK phosphorylation in the whole hypothalamus. However, our findings provide the
345 first demonstration that basal AMPK phosphorylation in the nodose ganglion of HFD-fed
346 mice was significantly higher than that of CD-fed mice. The higher basal AMPK
347 phosphorylation in skeletal muscle of DIO mice is thought to contribute to leptin resistance
348 (Martin *et al*. 2006). The pathophysiological significance of altered AMPK phosphorylation
349 level and AMPK's role as the ghrelin signaling molecule in the nodose ganglion should be
350 investigated in future work.

351 Briggs *et al.* (Briggs *et al.* 2014) recently showed that 3-week HFD–induced
352 hyperleptinemia (~7 ng/ml) can cause ghrelin resistance. Furthermore, they observed
353 hypothalamic gliosis, as revealed by increases in the numbers of glial fibrillary acidic
354 protein–positive glia and their projections. They explained the ghrelin resistance under 3-
355 week HFD as a consequence of leptin's counteracting effect against ghrelin on hypothalamic
356 NPY/AgRP neurons. We detected marked hyperleptinemia (89 ng/ml) in this study, in which
357 leptin did not exert an effect as an anorectic protein, as reported in many investigations (El-
358 Haschimi *et al.* 2000, Zhang *et al*. 2008). Short-term HFD could cause ghrelin resistance in
359 the hypothalamus via hyperleptinemia; however, we believed that long-term HFD causes
360 ghrelin resistance via chronic inflammation in the nodose ganglion and hypothalamus.

361 Ghrelin modulates immune processes by both suppressing sympathetic nerve activity
362 and reducing inflammatory cytokine production in activated macrophages (Dixit *et al.* 2004).

The vagal efferent nerve activity was reduced in obese patients, and selective cholinergic activation of the vagal efferent nerve in DIO mice suppressed obesity-related inflammation and restored metabolic complications (Pavlov and Tracey 2012). Berkseth *et al*. recently showed that 4-week CD (12 kilocalories from fat) following 16-week HFD (60% kilocalories from fat) given to C57BL/6 mice reversed hypothalamic inflammation (Berkseth *et al*. 2014). A future study may delineate whether inflammation in the nodose ganglion and ghrelin resistance caused by HFD are also reversible after switching to a low-fat diet.

In conclusion, this study offers the first evidence that HFD causes inflammatory responses in the nodose ganglion in addition to the hypothalamus. Additionally, ghrelin resistance in obese states could be associated with inflammation in the nodose ganglion. The vagal afferent nerve may act as a novel pathway that mediates the peripheral inflammatory signal to the brain.

Declaration of interest

The authors declare that there is no conflict of interest that could be perceived as prejudicing the impartiality of the research reported.

Funding

This work was supported in part by JSPS KAKENHI (No. 25293216) and A-MED CREST to M.N.

Author contribution statement

F N, K T, H S, and M N designed the experiments; F N, K T, Z W, C N, and A M performed the experiments; F N, K T, and C N analyzed the data. All authors prepared and approved the final version of the manuscript.

Acknowledgment

The authors thank Sumie Tajiri (University of Miyazaki) for technical support.

5. References

Andrews ZB, Erion DM, Beiler R, Choi CS, Shulman GI & Horvath TL 2010 Uncoupling protein-2 decreases the lipogenic actions of ghrelin. *Endocrinology* **151** 2078-2086.

Berkseth KE, Guyenet SJ, Melhorn SJ, Lee D, Thaler JP, Schur EA & Schwartz MW 2014 Hypothalamic gliosis associated with high-fat diet feeding is reversible in mice: a combined immunohistochemical and magnetic resonance imaging study. *Endocrinology* **155** 2858-2867.

Briggs DI, Enriori PJ, Lemus MB, Cowley MA & Andrews ZB 2010 Diet-induced obesity causes ghrelin resistance in arcuate NPY/AgRP neurons. *Endocrinology* **151** 4745-4755.

Briggs DI, Lockie SH, Benzler J, Wu Q, Stark R, Reichenbach A, Hoy AJ, Lemus MB, Coleman HA, Parkington HC *et al.* 2014 Evidence that diet-induced hyperleptinemia, but not hypothalamic gliosis, causes ghrelin resistance in NPY/AgRP neurons of male mice. *Endocrinology* **155** 2411-2422.

Cai D & Liu T 2011 Hypothalamic inflammation: a double-edged sword to nutritional diseases. *Annals of the New York Academy of Sciences* **1243** E1-39.

Daly DM, Park SJ, Valinsky WC & Beyak MJ 2011 Impaired intestinal afferent nerve satiety signalling and vagal afferent excitability in diet induced obesity in the mouse. *Journal of Physiology* **589** 2857-2870.

Date Y, Murakami N, Toshinai K, Matsukura S, Niijima A, Matsuo H, Kangawa K & Nakazato M 2002 The role of the gastric afferent vagal nerve in ghrelin-induced feeding and growth hormone secretion in rats. *Gastroenterology* **123** 1120-1128.

Date Y, Shimbara T, Koda S, Toshinai K, Ida T, Murakami N, Miyazato M, Kokame K, Ishizuka Y, Ishida Y *et al.* 2006 Peripheral ghrelin transmits orexigenic signals through the noradrenergic pathway from the hindbrain to the hypothalamus. *Cell*

Metabolism **4** 323-331.

Date Y, Toshinai K, Koda S, Miyazato M, Shimbara T, Tsuruta T, Niijima A, Kangawa K & Nakazato M 2005 Peripheral interaction of ghrelin with cholecystokinin on feeding regulation. *Endocrinology* **146** 3518-3525.

de La Serre CB, Ellis CL, Lee J, Hartman AL, Rutledge JC & Raybould HE 2010 Propensity to high-fat diet-induced obesity in rats is associated with changes in the gut microbiota and gut inflammation. *American Journal of Physiology Gastrointestinal and Liver Physiology* **299** G440-448.

de Lartigue G, Barbier de la Serre C, Espero E, Lee J & Raybould HE 2011 Diet-induced obesity leads to the development of leptin resistance in vagal afferent neurons. *American Journal of Physiology Endocrinology and Metabolism* **301** E187-195.

De Souza CT, Araujo EP, Bordin S, Ashimine R, Zollner RL, Boschero AC, Saad MJ & Velloso LA 2005 Consumption of a fat-rich diet activates a proinflammatory response and induces insulin resistance in the hypothalamus. *Endocrinology* **146** 4192-4199.

Dixit VD, Schaffer EM, Pyle RS, Collins GD, Sakthivel SK, Palaniappan R, Lillard JW, Jr. & Taub DD 2004 Ghrelin inhibits leptin- and activation-induced proinflammatory cytokine expression by human monocytes and T cells. *Journal of Clinical Investigation* **114** 57-66.

El-Haschimi K, Pierroz DD, Hileman SM, Bjorbaek C & Flier JS 2000 Two defects contribute to hypothalamic leptin resistance in mice with diet-induced obesity. *Journal of Clinical Investigation* **105** 1827-1832.

Gardiner JV, Campbell D, Patterson M, Kent A, Ghatei MA, Bloom SR & Bewick GA 2010 The hyperphagic effect of ghrelin is inhibited in mice by a diet high in fat. *Gastroenterology* **138** 2468-2476.

Goehler LE, Gaykema RP, Nguyen KT, Lee JE, Tilders FJ, Maier SF & Watkins LR 1999

Interleukin-1beta in immune cells of the abdominal vagus nerve: a link between the immune and nervous systems? *Journal of Neuroscience* **19** 2799-2806.

Gutkind JS 2000 Regulation of mitogen-activated protein kinase signaling networks by G protein-coupled receptors. *Science's STKE* **2000** re1.

Henkel JS, Beers DR, Siklós L & Appel SH 2006 The chemokine MCP-1 and the dendritic and myeloid cells it attracts are increased in the mSOD1 mouse model of ALS. *Molecular and Cellular Neuroscience* **31** 427-437.

Hosoi T, Okuma Y, Matsuda T & Nomura Y 2005 Novel pathway for LPS-induced afferent vagus nerve activation: possible role of nodose ganglion. *Autonomic Neuroscience* **120** 104-107.

Hotamisligil GS, Shargill NS & Spiegelman BM 1993 Adipose expression of tumor necrosis factor-alpha: direct role in obesity-linked insulin resistance. *Science* **259** 87-91.

Ito D, Imai Y, Ohsawa K, Nakajima K, Fukuuchi Y & Kohsaka S 1998 Microglia-specific localisation of a novel calcium binding protein, Iba1. *Molecular Brain Research* **57** 1-9.

Kojima M, Hosoda H, Date Y, Nakazato M, Matsuo H & Kangawa K 1999 Ghrelin is a growth-hormone-releasing acylated peptide from stomach. *Nature* **402** 656-660.

Kola B, Hubina E, Tucci SA, Kirkham TC, Garcia EA, Mitchell SE, Williams LM, Hawley SA, Hardie DG, Grossman AB *et al.* 2005 Cannabinoids and Ghrelin Have Both Central and Peripheral Metabolic and Cardiac Effects via AMP-activated Protein Kinase. *Journal of Biological Chemistry* **280** 25196-25201.

Konturek SJ, Konturek JW, Pawlik T & Brzozowski T 2004 Brain-gut axis and its role in the control of food intake. *Journal of Physiology and Pharmacology* **55** 137-154.

Martin TL, Alquier T, Asakura K, Furukawa N, Preitner F & Kahn BB 2006 Diet-induced Obesity Alters AMP Kinase Activity in Hypothalamus and Skeletal Muscle. *Journal*

of Biological Chemistry **281** 18933-18941.

McFarlane MR, Brown MS, Goldstein JL & Zhao TJ 2014 Induced ablation of ghrelin cells in adult mice does not decrease food intake, body weight, or response to high-fat diet. *Cell Metabolism* **20** 54-60.

Milanski M, Degasperi G, Coope A, Morari J, Denis R, Cintra DE, Tsukumo DM, Anhe G, Amaral ME, Takahashi HK *et al.* 2009 Saturated fatty acids produce an inflammatory response predominantly through the activation of TLR4 signaling in hypothalamus: implications for the pathogenesis of obesity. *Journal of Neuroscience* **29** 359-370.

Minokoshi Y, Alquier T, Furukawa N, Kim Y-B, Lee A, Xue B, Mu J, Foufelle F, Ferre P, Birnbaum MJ *et al.* 2004 AMP-kinase regulates food intake by responding to hormonal and nutrient signals in the hypothalamus. *Nature* **428** 569-574.

Mousseaux D, Le Gallic L, Ryan J, Oiry C, Gagne D, Fehrentz JA, Galleyrand JC & Martinez J 2006 Regulation of ERK1/2 activity by ghrelin-activated growth hormone secretagogue receptor 1A involves a PLC/PKCε pathway. *British Journal of Pharmacology* **148** 350-365.

Nakazato M, Murakami N, Date Y, Kojima M, Matsuo H, Kangawa K & Matsukura S 2001 A role for ghrelin in the central regulation of feeding. *Nature* **409** 194-198.

Pavlov VA & Tracey KJ 2012 The vagus nerve and the inflammatory reflex−linking immunity and metabolism. *Nature Reviews Endocrinology* **8** 743-754.

Perego C, Fumagalli S & De Simoni MG 2011 Temporal pattern of expression and colocalization of microglia/macrophage phenotype markers following brain ischemic injury in mice. *Journal of Neuroinflammation* **8** 174.

Perreault M, Istrate N, Wang L, Nichols AJ, Tozzo E & Stricker-Krongrad A 2004 Resistance to the orexigenic effect of ghrelin in dietary-induced obesity in mice: reversal upon weight loss. *International Journal of Obesity and Related Metabolic Disorders* **28**

879-885.

Posey KA, Clegg DJ, Printz RL, Byun J, Morton GJ, Vivekanandan-Giri A, Pennathur S, Baskin DG, Heinecke JW, Woods SC *et al.* 2009 Hypothalamic proinflammatory lipid accumulation, inflammation, and insulin resistance in rats fed a high-fat diet. *American Journal of Physiology Endocrinology and Metabolism* **296** E1003-1012.

Rinaman L 2010 Ascending projections from the caudal visceral nucleus of the solitary tract to brain regions involved in food intake and energy expenditure. *Brain Research* **1350** 18-34.

Schenk S, Saberi M & Olefsky JM 2008 Insulin sensitivity: modulation by nutrients and inflammation. *Journal of Clinical Investigation* **118** 2992-3002.

Shiiya T, Nakazato M, Mizuta M, Date Y, Mondal MS, Tanaka M, Nozoe S, Hosoda H, Kangawa K & Matsukura S 2002 Plasma ghrelin levels in lean and obese humans and the effect of glucose on ghrelin secretion. *Journal of Clinical Endocrinology and Metabolism* **87** 240-244.

Thaler JP, Guyenet SJ, Dorfman MD, Wisse BE & Schwartz MW 2013 Hypothalamic inflammation: marker or mechanism of obesity pathogenesis? *Diabetes* **62** 2629-2634.

Thaler JP, Yi CX, Schur EA, Guyenet SJ, Hwang BH, Dietrich MO, Zhao X, Sarruf DA, Izgur V, Maravilla KR *et al.* 2012 Obesity is associated with hypothalamic injury in rodents and humans. *Journal of Clinical Investigation* **122** 153-162.

Toshinai K, Date Y, Murakami N, Shimada M, Mondal MS, Shimbara T, Guan JL, Wang QP, Funahashi H, Sakurai T *et al*. 2003 Ghrelin-induced food intake is mediated via the orexin pathway. *Endocrinology* **144** 1506-1512.

Tschöp M, Weyer C, Tataranni PA, Devanarayan V, Ravussin E & Heiman ML 2001 Circulating ghrelin levels are decreased in human obesity. *Diabetes* **50** 707-709.

Zhang X, Zhang G, Zhang H, Karin M, Bai H & Cai D 2008 Hypothalamic IKKbeta/NF-

kappaB and ER stress link overnutrition to energy imbalance and obesity. *Cell* **135** 61-73.

Zhuo H, Ichikawa H & Helke CJ 1997 Neurochemistry of the nodose ganglion. *Progress in Neurobiology* **52** 79-107.

Figure legends

Figure 1 Effects of ghrelin on food intake (A, B, and C), and oxygen consumption (D, E, and F) of mice fed a CD or a HFD for 12 weeks. Two-hour food intake during the light phase in response to s.c. (A) or i.c.v. (B) administration of ghrelin, and dark-phase food intake (C) in response to i.c.v. administration of NRS IgG or anti-ghrelin IgG, in CD- or HFD-fed mice. Oxygen consumptions in CD- (D) or HFD-fed mice (E) subjected to s.c. ghrelin administration, and AUC of oxygen consumption from 0 to 2 h after ghrelin administration (F). Dark-phase food intake of CD- or HFD-fed mice subjected to leptin administration (G). NS, not significant. Values are means ± SEM. **P* < 0.05, ***P* < 0.01.

Figure 2 Time course of plasma ghrelin concentrations after s.c. administration to CD- or HFD-fed mice. Values are means ± SEM.

Figure 3 Electrophysiological effect of ghrelin on gastric vagal afferent activity in CD- or HFD-fed mice. Representative data of gastric vagal afferent discharge rates are shown in A–D. Gastric vagal afferent discharge in CD-fed mice was not affected by s.c. administration of saline (A), whereas it was inhibited by administration of ghrelin (B). Gastric vagal afferent discharge in HFD-fed mice was not affected by neither saline (C) nor ghrelin (D). E, Ghrelin significantly attenuated impulses 10 min after its injection in CD- but not HFD-fed mice. **P* < 0.05 vs. CD-fed mice subjected to saline injection. NS, not significant.

Figure 4 Representative Fos expression patterns in hypothalamic arcuate nucleus in response to s.c. administration of saline (A) or ghrelin (B) in CD-fed mice and saline (C) or ghrelin (D) in HFD-fed mice. Fos expression patterns in the arcuate nucleus in response to i.c.v. administration of aCSF (E) or ghrelin (F) in CD-fed mice and aCSF (G) or ghrelin (H) in

546 HFD-fed mice. Numbers of Fos-immunoreactive neurons of mice subjected to s.c. (I) or i.c.v.
547 administration (J) of ghrelin or vehicle. Values are means ± SEM. **P* < 0.05 vs. saline or
548 aCSF. Scale bars, 50 μm.
549
550 **Figure 5** mRNA expressions of *Ghsr* in the nodose ganglion and hypothalamus of CD- or
551 HFD-fed mice. Values are means ± SEM. **P* < 0.05 vs CD.
552
553 **Figure 6** mRNA expression of *Tlr4* (A) and *Tlr2* (B) in the nodose ganglion and
554 hypothalamus of CD- or HFD-fed mice. Expressions of genes encoding macrophage markers
555 (*Iba1* and *Emr1*) and inflammatory cytokines (*Il-1b*, *Il-6*, and *Tnfα*) in the nodose ganglion
556 (C) and hypothalamus (D) of CD- or HFD-fed mice. mRNAs were quantitated relative to
557 *Gapdh* or *Tbp* housekeeping gene, and relative levels are presented as fold change relative to
558 CD. Values are means ± SEM. **P* < 0.05, ***P* < 0.01 vs CD. Histochemical analyses of HFD-
559 induced macrophage accumulation in the nodose ganglion and hypothalamus.
560 Immunohistochemical detection of Iba1 (E and F) and CD11b (G and H) in the nodose
561 ganglion and Iba1 (I and J) and CD11b (K and L) in the hypothalamus of CD- or HFD-fed
562 mice. Numbers of cells stained with Iba1 or CD11b antibody in the nodose ganglion (M) and
563 hypothalamus (N). Values are means ± SEM. **P* < 0.05, ***P* < 0.01 vs CD. Scale bars, 50 μm
564
565 **Figure 7** Immunohistochemical analyses of HFD-induced M1 macrophage accumulation in
566 the nodose ganglion and hypothalamus. Iba1, CD86, and merged images in the nodose
567 ganglion (A, B, C, D, E, and F), and the hypothalamus (G, H, I, J, K, and L) of CD- or HFD-
568 fed mice. Arrows indicate co-localization of CD86 with Iba1. The insets in C, F, I, and L are
569 higher magnification examples of $Iba1^{+}/CD86^{+}$ cells. Numbers of cells stained with Iba1 or
570 CD86 antibody in the nodose ganglion (M) and hypothalamus (N). Values are means ± SEM.

571 *$P < 0.05$ vs. CD. Scale bars, 50 μm.

572

573 **Figure 8** Representative Western blots for pERK1/2 and ERK1/2 in the nodose ganglion of
574 CD- and HFD-fed mice (A). Levels of basal phosphorylation of ERK1 and ERK2 in the
575 nodose ganglion of CD- and HFD-fed mice (B). Phosphorylated ERK1 and ERK2 in the
576 nodose ganglion after s.c. administration of ghrelin (C). GAPDH was used as a control.
577 Values are means ± SEM and represent the ratio of the intensity of bands corresponding to
578 pERK1 and ERK1 or pERK2 and ERK2. *$P < 0.05$ vs saline.

579

580 **Figure 9** Representative Western blots for pAMPKα and AMPKα in the nodose ganglion of
581 CD- or HFD-fed mice (A). Ghrelin promoted phosphorylation of AMPKα in CD- but not in
582 HFD-fed mice (B). GAPDH was used as a control. Values are means ± SEM and represent
583 the ratio of the intensity of bands corresponding to pAMPK and AMPK. *$P < 0.05$ vs saline.

Table 1

Characteristics and blood parameters of mice fed a CD or a HFD

	CD	HFD
Initial body weight (g)	23.9 ± 0.6	24.2 ± 0.6
Final body weight (g)	30.2 ± 0.4	49.6 ± 0.9***
Epididymal fat weight (g)	0.54 ± 0.01	2.59 ± 0.24***
24-h food intake (g)	3.27 ± 0.07	2.62 ± 0.04***
24-h energy intake (kJ)	46.5 ± 1.0	57.4 ± 0.8***
Blood glucose (mmol/l)	6.5 ± 0.3	9.8 ± 0.7*
Plasma insulin (ng/ml)	0.35 ± 0.01	1.65 ± 0.09***
Plasma leptin (ng/ml)	6.1 ± 0.4	89.1 ± 5.6***
Plasma ghrelin (fmol/ml)	65.7 ± 9.9	8.8 ± 1.2**
Plasma des-acyl ghrelin (fmol/ml)	1,255 ± 157	937 ± 54*

Data are expressed as means ± SEM (n = 6 – 8). *P < 0.05, **P < 0.01, ***P < 0.001 vs CD.

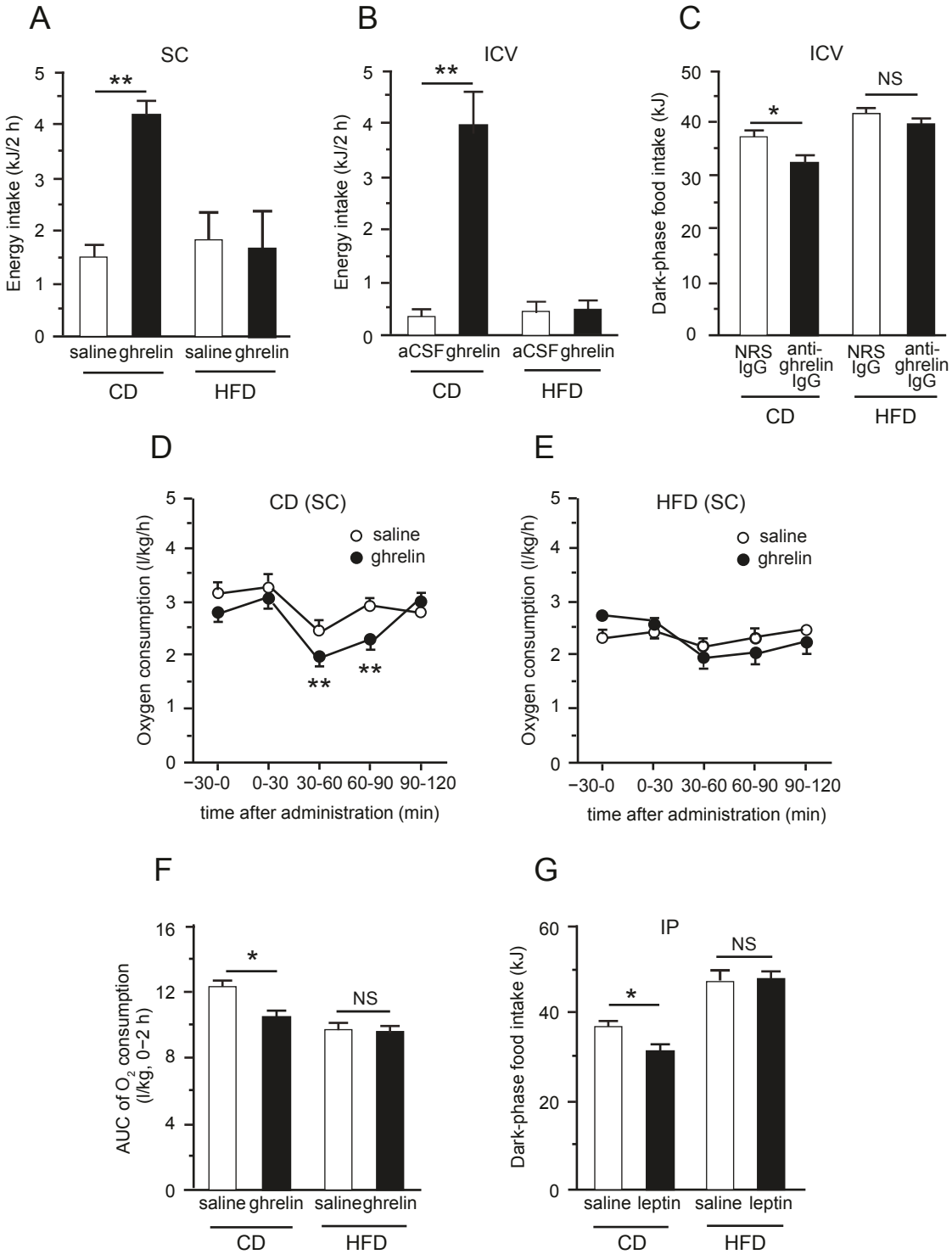

Fig. 1. Naznin *et al.*

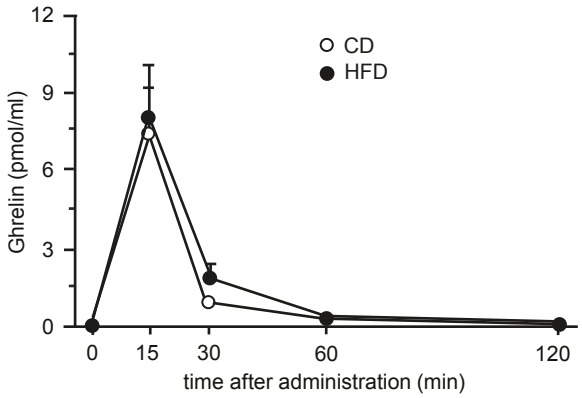

Fig. 2. Naznin *et al.*

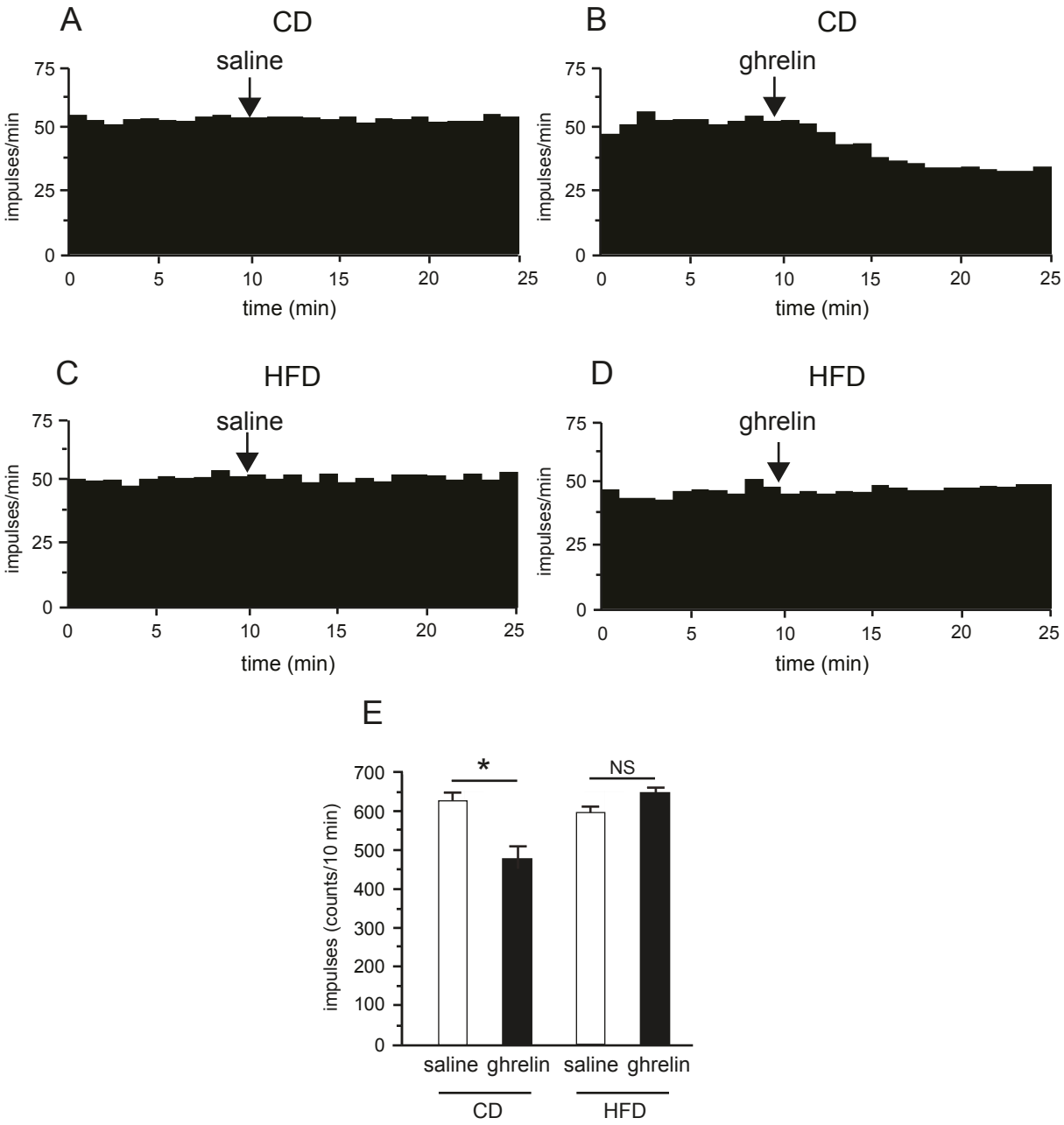

Fig. 3. Naznin *et al.*

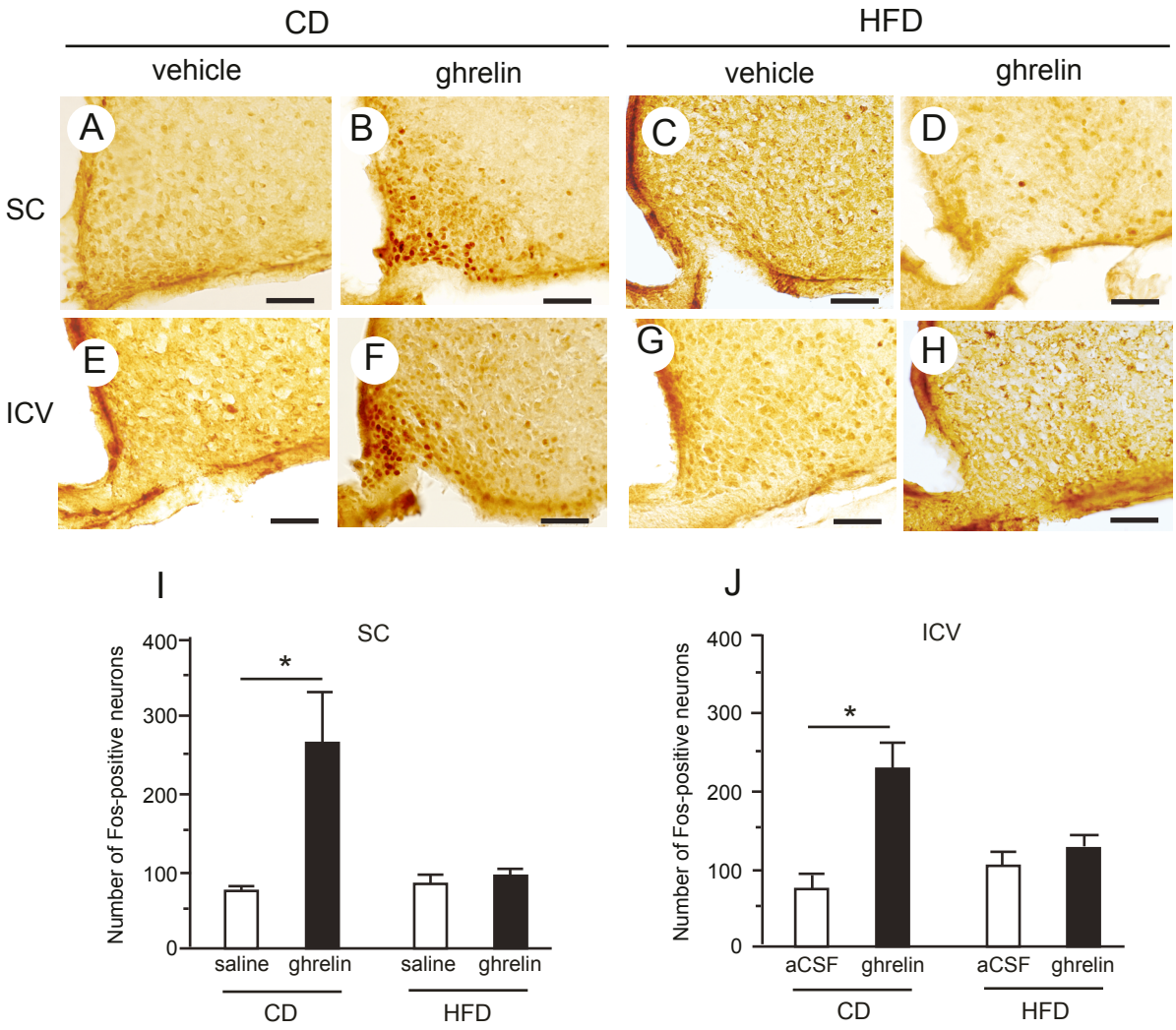

Fig. 4. Naznin *et al.*

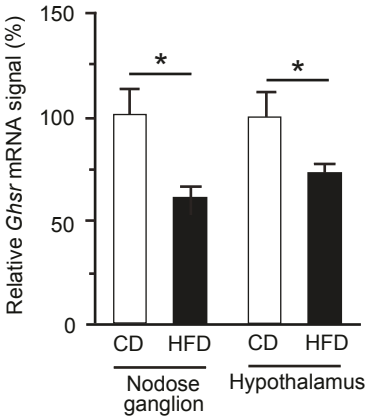

Fig. 5. Naznin *et al.*

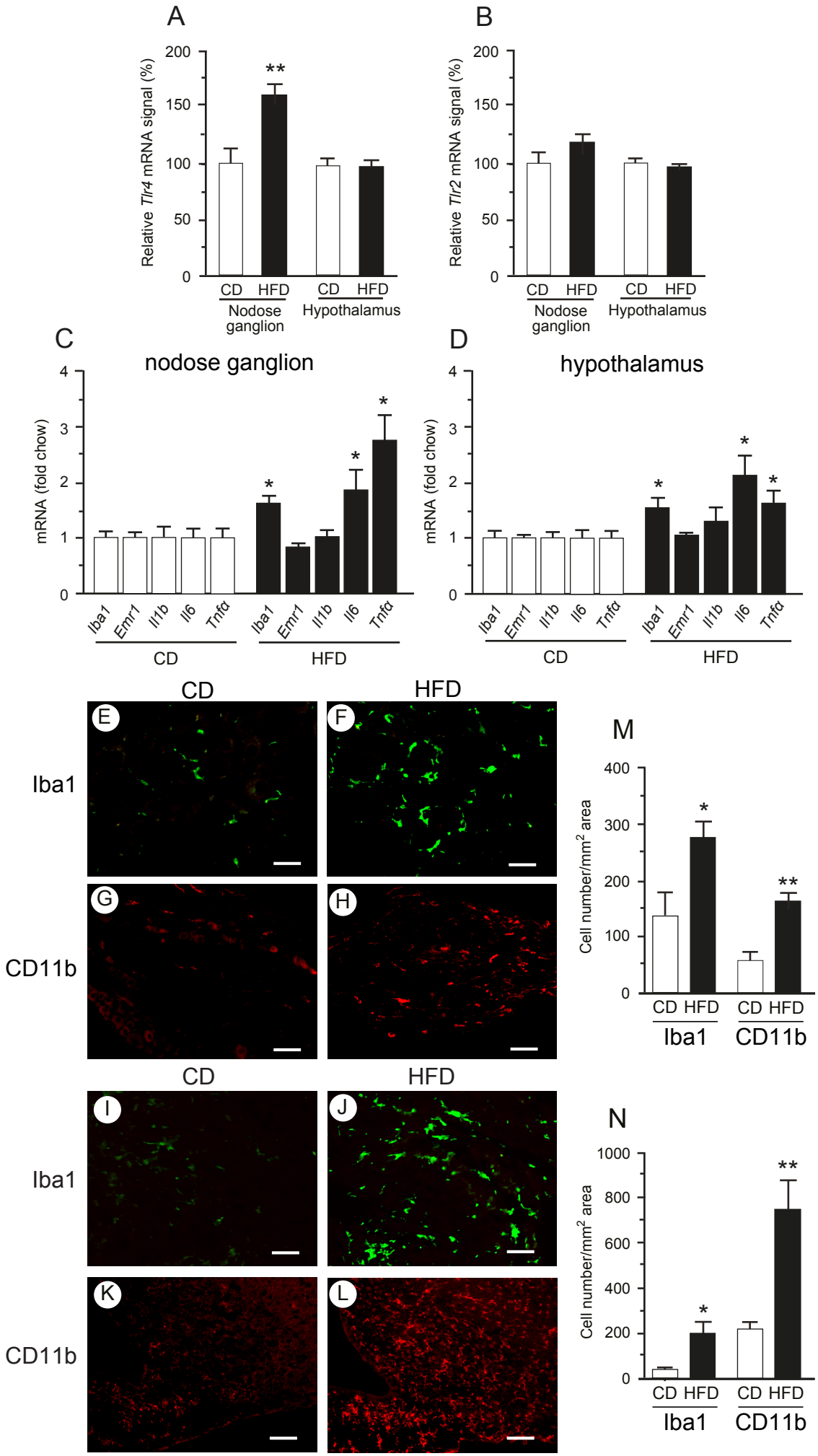

Fig. 6. Naznin *et al.*

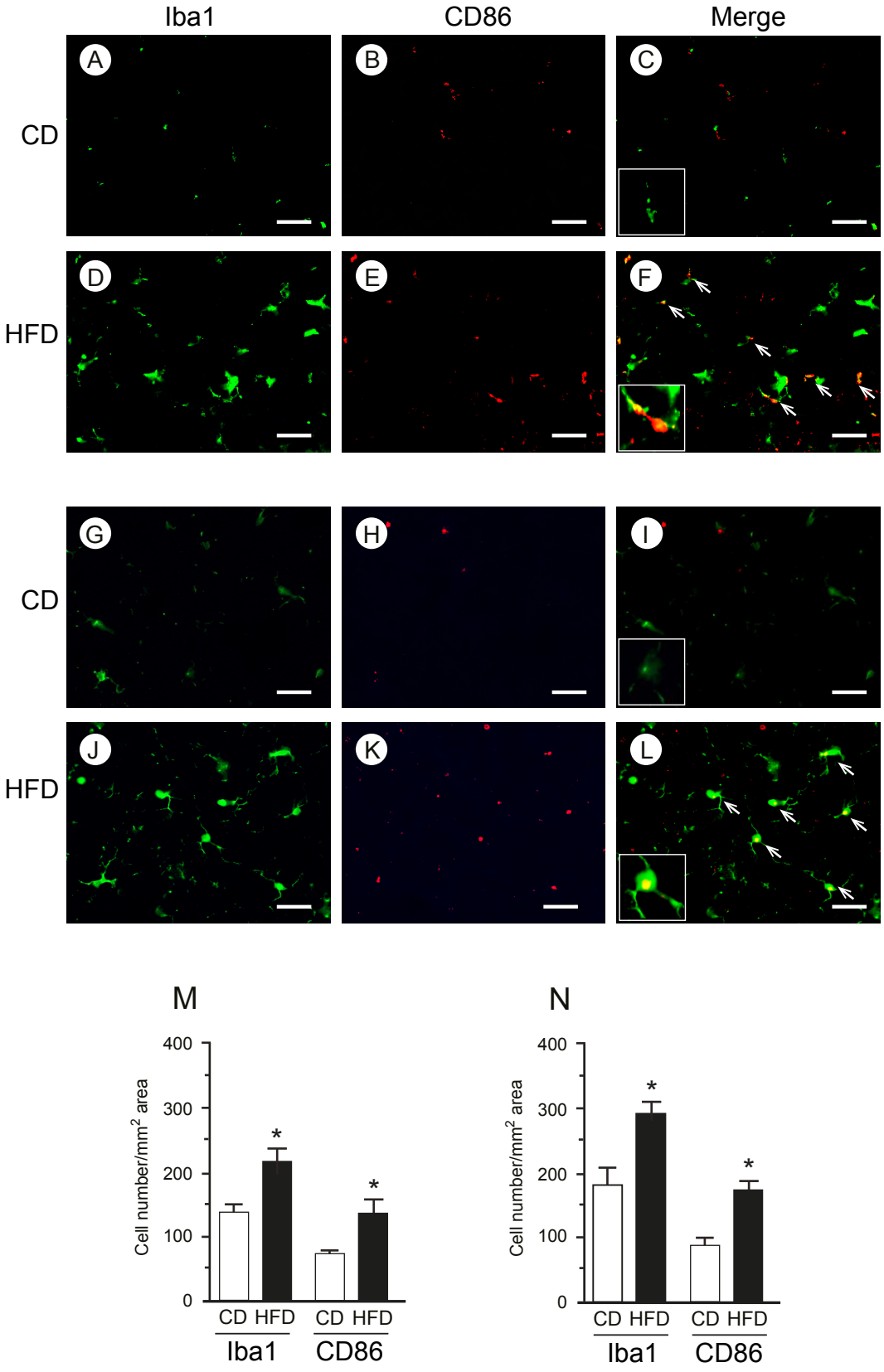

Fig. 7. Naznin *et al.*

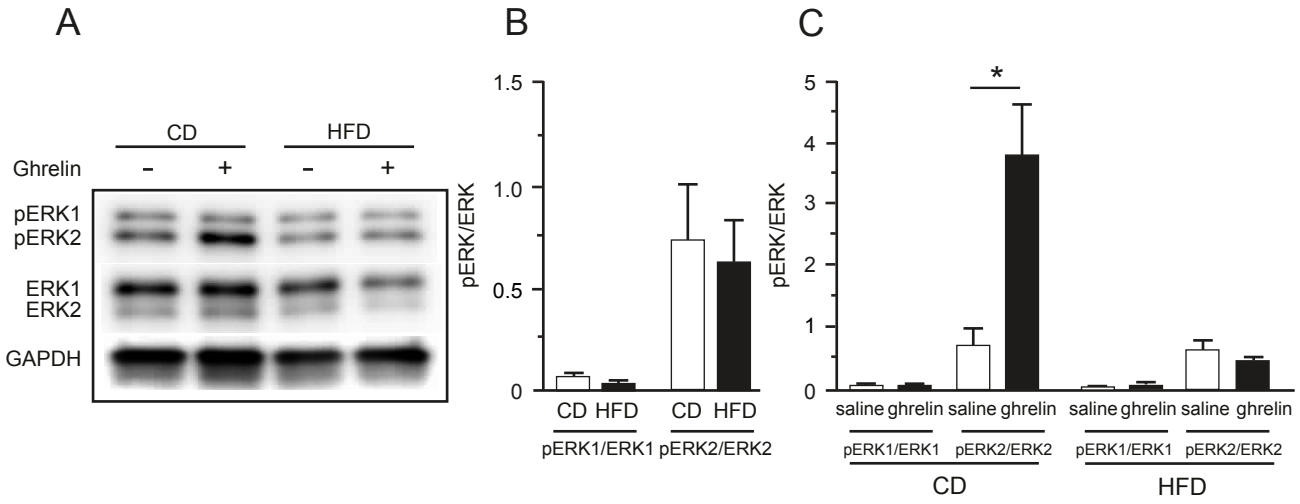

Fig. 8. Naznin *et al.*

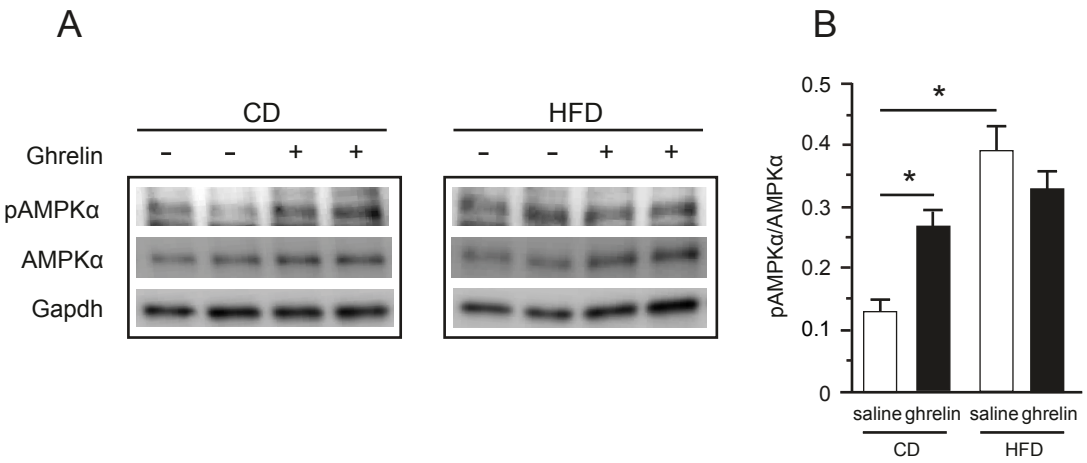

Fig. 9. Naznin *et al.*